Special Issue

Breaking Symmetry Relaxes Structural and Magnetic Restraints, Suppressing QTM in Enantiopure Butterfly Fe_2Dy_2 SMMs**

Amer Baniodeh,*[a, b] Danny Wagner,[c] Yan Peng,[a, b] Hagen Kaemmerer,[a, d] Nicolas Leblanc,[b] Stefan Bräse,[c, e] Jean-Valére Naubron,[f] Christopher E. Anson,[a] and Annie K. Powell*[a, b, d]

Abstract: The $\{Fe_2Dy_2\}$ butterfly systems can show single molecule magnet (SMM) behaviour, the nature of which depends on details of the electronic structure, as previously demonstrated for the $[Fe_2Dy_2(\mu_3\text{-}OH)_2(Me\text{-}teaH)_2(O_2CPh)_6]$ compound, where the [N,N-bis-(2-hydroxyethyl)-amino]-2-propanol (Me-$teaH_3$) ligand is usually used in its racemic form. Here, we describe the consequences for the SMM properties by using enantiopure versions of this ligand and present the first homochiral 3d/4f SMM, which could only be obtained for the *S* enantiomer of the ligand for $[Fe_2Dy_2(\mu_3\text{-}OH)_2(Me\text{-}teaH)_2(O_2CPh)_6]$ since the *R* enantiomer underwent significant racemisation. To investigate this further, we prepared the $[Fe_2Dy_2(\mu_3\text{-}OH)_2(Me\text{-}teaH)_2(O_2CPh)_4(NO_3)_2]$ version, which could be obtained as the *RS*-, *R*- and *S*-compounds. Remarkably, the enantiopure versions show enhanced slow relaxation of magnetisation. The use of the enantiomerically pure ligand suppresses QTM, leading to the conclusion that use of enantiopure ligands is a "gamechanger" by breaking the cluster symmetry and altering the intimate details of the coordination cluster's molecular structure.

Introduction

Symmetry and the implied chirality of many systems is a fundamental detail in our daily life. For example, this article has been written with help of chiral instruments (right and left hands) in combination with keys on the keyboard. Had it been written using a pen then it would have been written homochirally, and the majority of authors would have chosen their naturally more adept right hand. The effect of "handedness" is also obvious to us with our experience of many familiar chemical substances which we recognise as having different colours, smells, tastes and sometimes dramatic effects on our health as a result of their different absolute configurations. Our natural environment is also full of examples of chirality. Snails which have chiral spiral shells are famously found with a predominance of the right-handed versions. Such details concerning chirality increasingly fascinate chemists and physicists in areas as diverse as the synthesis of new compounds to deeper questions regarding the electronic and magnetic behaviour of fundamental particles. A meeting point of these areas is provided by the systems which are described as molecular magnets. Indeed, when magnetism and chirality shake hands this leads to a variety of unexpected phenomena such as large magnetochiral effects.[1]

Given some recent results[2] we published on the unexpected ability of some Fe^{III}/4f cyclic coordination cluster systems

[a] Dr. A. Baniodeh, Dr. Y. Peng, H. Kaemmerer, Dr. C. E. Anson, Prof. A. K. Powell
Institute of Inorganic Chemistry
Karlsruhe Institute of Technology
Engesserstr. 15, 76131 Karlsruhe (Germany)
E-mail: dramer.baniodeh@gmail.com
annie.powell@kit.edu

[b] Dr. A. Baniodeh, Dr. Y. Peng, Dr. N. Leblanc, Prof. A. K. Powell
Institute for Nanotechnology (INT)
Karlsruhe Institute of Technology
Hermann-von-Helmholtz-Platz 1
76344 Eggenstein-Leopoldshafen (Germany)

[c] D. Wagner, Prof. S. Bräse
Institute of Organic Chemistry
Karlsruhe Institute of Technology
Fritz-Haber-Weg 6, 76131 Karlsruhe (Germany)

[d] H. Kaemmerer, Prof. A. K. Powell
Institute for Quantum Materials and Technologies (IQMT)
Karlsruhe Institute of Technology
Hermann-von-Helmholtz-Platz 1
76344 Eggenstein-Leopoldshafen (Germany)

[e] Prof. S. Bräse
Institute of Biological and Chemical Systems (IBCS-FMS)
Karlsruhe Institute of Technology
Hermann-von-Helmholtz-Platz 1
76344 Eggenstein-Leopoldshafen (Germany)

[f] Dr. J.-V. Naubron
Aix Marseille Univ, CNRS, Centrale Marseille
Spectropole-FR1739,
Marseille (France)

[**] QTM = Quantum Tunnelling of Magnetisation, SMM = single molecule magnet.

Supporting information for this article is available on the WWW under https://doi.org/10.1002/chem.202103360

This manuscript is part of a Special Issue "Cooperative effects in heterometallic complexes".

to effect chiral separations of the racemic version of the methyl substituted triethanolamine ligand Me-teaH$_3$ (1-[N,N-bis-(2-hydroxyethyl)-amino]-2-propanol, Scheme 1) using an {Fe_2Yb_2} compound as a starting material, we wanted to explore the outcome of the reactions using enantiopure Me-teaH$_3$ ligand on the Fe_2Dy_2 SMM analogue. Two important aspects to this endeavour can be noted here. Firstly, access to the enantiopure versions of the ligands is not always straightforward and demands considerable synthetic expertise. Secondly, as Flack points out,[3] enantiopure molecules can only crystallise in chiral crystal structures. This in itself does not imply that the space group has to be chiral, but the obvious requirement is the lack of any inversion or mirror symmetry element. There are only 65 so-called Sohncke space groups compatible with this requirement, which are sometimes incorrectly referred to as "chiral" space groups. These 65 groups are further divided into 11 pairs of enantiomorphous chiral space groups, pairs such as $P6_1$ and $P6_5$ which are mirror images of each other in complete analogy with what is required for enantiomers of chiral molecules. The remaining 43 space groups with no enantiomeric pairs, such as P1, P2, P3, are thus correctly referred to as achiral.[3]

In order to test the influence of this type of {Fe_2Ln_2} coordination cluster on the local stereochemistry we chose the robust **[Fe_2Dy_2(μ_3-OH)$_2$(*R,S*-Me-teaH)$_2$(O_2CPh)$_6$]** coordination cluster, which is isostructural with the {Fe_2Yb_2} compound as a test-bed. This {Fe_2Dy_2} core structure is recognised to be a very stable motif.[4]

Results and Discussion

Crystallography

[Fe_2Dy_2(μ_3-OH)$_2$(*R,S*-Me-teaH)$_2$(O_2CPh)$_6$]·2PhCO$_2$H·4MeCN (1-RS) obtained with the racemic *R,S*-ligand

Crystals form over about one day in high yield. The centrosymmetric compound crystallises in $P\bar{1}$ with Z = 1.[+] The inversion centre thus relates the *R* and *S* ligands within the molecule. Although for situations like this, where the two halves of the molecule are related by an inversion centre it is common to observe disorder of *R* and *S* forms on each ligand, this is not the case here and perfect separation of *R* and *S* is achieved within the molecule.

The Me-teaH^{2-} ligand chelates with the protonated alcohol arm, which is the one bearing the methyl group and thus the chiral carbon, coordinated exclusively to the Dy^{III} ions. The two deprotonated (alkoxy) arms bridge between the outer Dy^{III} ions to the central two Fe^{III} ions and the metals are also bridged by two μ_3-OH units to give the {Fe_2Dy_2} core motif (Figure 1). The conformation of the three arms of the Me-teaH^{2-} ligand is very similar to that in the previously reported teaH^{2-} analogues.[4a,c,5] Four benzoate form *syn-syn* bridges between the "body" Fe ions (six coordinate) and the "wingtip" Dy ions of the butterfly core. The Dy coordination spheres are completed by one chelating benzoate each and are thus nine coordinate.

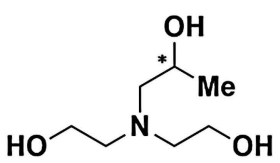

Scheme 1. The Me-teaH$_3$ ligand: [N,N-bis-(2-hydroxyethyl)-amino]-2-propanol with the chiral carbon marked with a star.

[Fe_2Dy_2(μ_3-OH)$_2$(*S*-Me-teaH)$_2$(O_2CPh)$_6$]·2PhCO$_2$H·4MeCN (1-SS) obtained with the enantiomerically-pure *S*-ligand

The compound also crystallises with Z = 1 in essentially the same triclinic unit cell as for the previous structure and with the same array of lattice solvent (4 MeCN + 2 PhCO$_2$H). The unit cell differs only slightly from that for compound **1** (Table S1).

The compound crystallises in the acentric space group P1, as indicated by the intensity statistics (mean value of $|E^2-1| = 0.766$). A whole sphere of data was collected and the solution and refinement in P1 yielded the structure of the complete Fe_2Dy_2 cluster and the lattice solvent. The correct assignment of the absolute configuration is confirmed by the Flack parameter $\chi = 0.047(5)$.[6] In fact this combination of the P1 space group, a zero Flack parameter and fully-ordered methyl groups excludes the possibility of twinned crystals having arisen from a racemic conglomerate, as illustrated in scheme S1.[7]

[Fe_2Dy_2(μ_3-OH)$_2$(*R*-Me-teaH)$_2$(O_2CPh)$_6$]·2PhCO$_2$H·4MeCN (1-RR) obtained with the enantiomerically-pure *R*-ligand

In attempting to make the corresponding **1-RR** enantiopure analogue, we found that there was a significant degree of ligand racemisation and a rather small yield. The reason remains unknown and this precluded using this compound for any magnetic studies. The partial racemisation of the ligands during the crystallisation of 1-RR resulted in a significantly higher level of pseudosymmetry than for the other enantiopure structures. Anisotropic refinement of all atoms required global rigid-bond restraints, and thus more restraints than parameters. It was therefore decided to refine the metal atoms anisotropically but to keep the lighter atoms isotropic. The structure is nonetheless reported here for completeness.

Comparison between the structures of 1-RS and 1-SS

At first sight, the molecular structures of compounds **1-RS** and **1-SS** appear to be identical, and the packing diagrams are also very similar (Figure 1). But looking at the molecular structure in more detail it is possible to "spot the difference" which is highlighted in the top panel of Figure 1. For compound **1-RS** the inversion-related *R* and *S* methyl-substituted arms are chelating the two wingtip Dy. In compound **1-SS**, which has no inversion centre, one of the two *S* arms is forced to adopt a bridging role which in turn means that one alkoxy arm has to take over its chelating role. This in turn requires that the *S* arm is now deprotonated and one of the non-substituted arms is now chelating and protonated. If we look at the space-filling representations of **1-RS** and **1-SS** (Figure S24), four of the six methylene hydrogens (coloured orange) in the teaH$_3$ ligands of the original [Fe_2Dy_2(μ_3-OH)$_2$(teaH)$_2$(O_2CPh)$_6$][8] compound cannot be replaced by a methyl group, since impossibly short intramolecular steric contacts would result. For the other two, one position, on the chelating arm is clearly favoured over the other

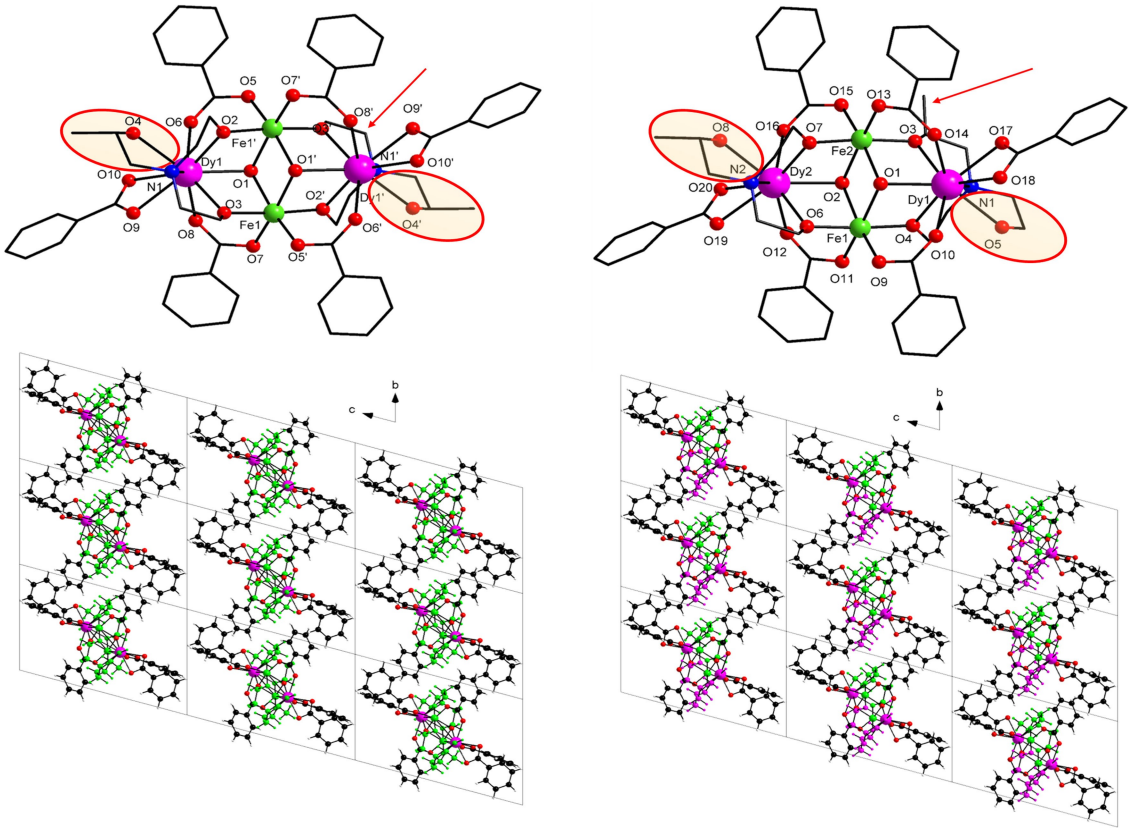

Figure 1. Molecular structures of the compound formed with the *R,S*-Me-teaH^{2-} (**1-RS**) and with the *S,S*-Me-teaH^{2-} (**1-SS**) ligand (top left and right). The respective packing shown in the lower panel. Although at a first glance the structures appear identical the top panel highlights the subtle changes resulting from the use of the enantiopure ligand. For compound **1-SS** on the right hand side of the molecule, compared with the situation for compound **1-RS**, the former chelating methyl alkoxy arm becomes a bridging arm whilst a former bridging alkoxy arm takes over the chelating function. Colour codes Dy: magenta, Fe: green, O: red, N: blue, C: black. In the lower panel in the left hand figure, both R and S ligand configuration are in green, i.e. are symmetry equivalent. In the right hand figure, the two different binding modes of the enantiopure ligand are highlighted by different colours (green and magenta).

and is adopted by both Me-teaH$_3$ ligands in **1-RS** (and **2-RS**), but the other, on a bridging arm, is still sterically possible and is adopted by one ligand in the enantiopure systems.

Thus, retaining the enantiopure *S*-configuration on the chiral arm of the ligand changes the intimate details of the molecular structure. Whereas the ligand on one side of the core structure (we have chosen this to be the left side of the molecule in Figure. 1) chelates with its chiral arm in exactly the same fashion as seen for compound **1-RS**, formed with the racemic ligand, the steric constraints on the left-hand side of the compound's core force the chiral arm to coordinate in a different way. In effect, this "unplugging and rewiring" of the ligand is illustrated in Scheme 2.

Although the breaking of the molecular centrosymmetry in **1-SS** is clearly real, the differences in coordination geometries between the pairs of metal centres that were equivalent in **1-RS** are in fact very small. A SHAPE[9] analysis (Table S3) shows that the deviations of the coordination polyhedra in **1-SS** from their idealised geometries are very similar (particularly for the two Dy) to those in **1-RS**. Comparison of the respective bond lengths within the Fe coordination polyhedra for **1-RS** and **1-SS** (Figure S8) shows that the differences here are small, and mostly not significant; if anything, the structures are more similar to each other than they both are to the analogue with (teaH)$^{2-}$ as ligand. Calculation of the theoretical coupling constants between the Fe centres from the bridging geometries in **1-RS** and **1-SS** using magnetostructural correlations[10] gave the same value ($J_{Fe\text{-}Fe} = -5.0$ cm^{-1}) in both cases, again emphasizing the similarity between the two structures.

The metal-metal distances are more precise than the M–O bond lengths, so these could allow a better estimate of any differences. In **1-RS**, Fe(1)··Fe(1′) is 3.2312(7) Å, while in **1-SS**, Fe(1)··Fe(2) is slightly larger at 3.2372(8) Å. Similarly, Fe(1)··Dy(1) and Fe(1)··Dy(1′) in **1-RS** are 3.4307(4) and 3.4209(4) Å, respectively, while in 1-SS the corresponding pairs of values are 3.4421(16) and 3.4379(16) Å and 3.4150816) and 3.4243(16) Å, respectively.

Magnetic studies

For compounds **1-RS** and **1-SS** the values of the χT products at 300 K are close to the expected values for the non-interacting metal ions. Both **1-RS** and **1-SS** show very similar steady decreases of their χT product values on decreasing the temperature from 300 to 1.8 K (Figure S10), suggesting that antiferro-

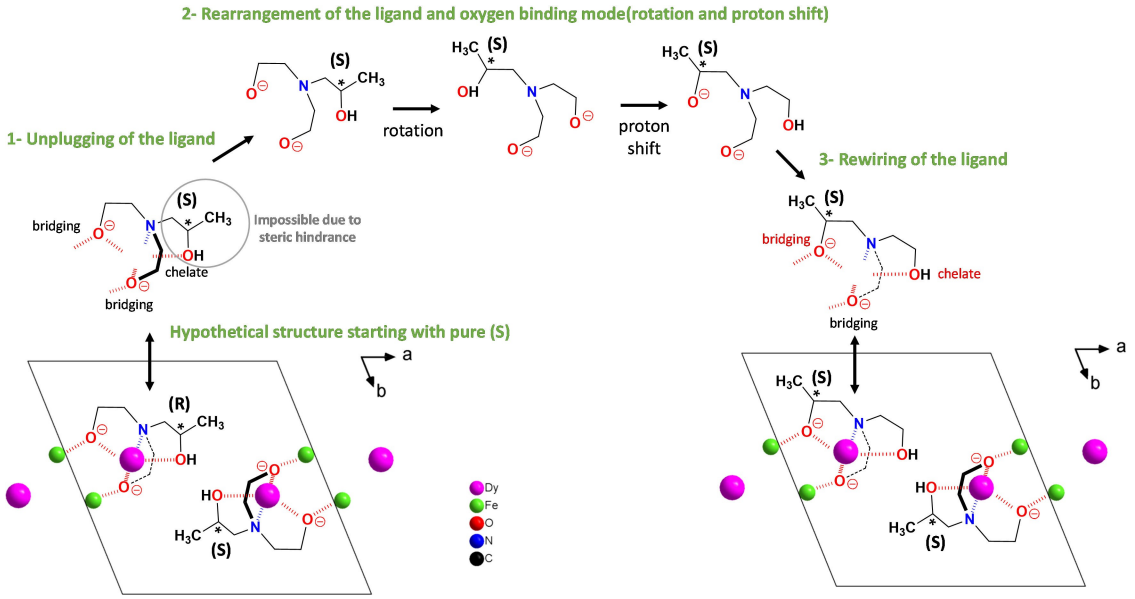

Scheme 2. Cartoon starting on the lower left from the compound 1 formed with the racemic version of the ligand to illustrate the unplugging, rearrangement and rewiring of one of the ligands when it is in its enantiopure form to give compound **1-SS** (lower right).

magnetic interactions between paramagnetic centres are present in these molecules as expected and shown for Fe_2Dy_2 systems in other studies.[4a,c,5] The field dependence of the magnetisation curves is shown in Figure S11. The magnetisation increases steadily upon application of an external field with no true saturation for either compound.

Although the static magnetism is very similar for both compounds, the dynamic properties show significant differences. To probe the relaxation *ac* magnetic susceptibility measurements were performed on **1-RS** and **1-SS**. The data are shown in Figure 2 together with the data we previously reported for the $teaH^{2-}$ analogue.[4a] Under zero *dc* field, for both the previously reported Fe_2Dy_2 compound with $teaH^{2-}$ and the racemic Me-$teaH^{2-}$ compound **1-RS** only weak out-of-phase components were detected. The in-phase components show insignificant frequency-dependence with no maxima. In contrast, the homochiral (*S,S*)-Fe_2Dy_2 compound **1-SS** shows a strong frequency-dependence for the in–phase signal, with a maximum at ca. 4 K. Strikingly, the out-of-phase component for compound **1-SS** shows up to a fourfold increase in intensity compared to **1-RS**. The χ''/χ' ratios are 0.025 ($teaH^{2-}$), 0.043 (**1-RS**), 0.667 (**1-SS**) underlining the fact that the SMM behaviour is significantly enhanced for the enantiopure compound **1-SS**.

Compound **1-RS** and its triethanolamine analogue[4a] show very similar and weak *ac* signals. Thus, the impressive enhancement seen for compound **1-SS** seems to be a direct consequence of removing the symmetry centre. One possibility could be fine tuning through moving the position of the methyl group on the right-hand side of compound **1-SS**. This possibility seems unlikely given the similarity of the relaxation behaviour for compound **1-RS** and the triethanolamine analogue.[4a]

Figure S13 illustrates the search for the optimised dc fields and Figure 3 shows the frequency-dependences of χ' and χ'' at temperatures from 1.9 to 5 K for **1-RS** and **1-SS** under their

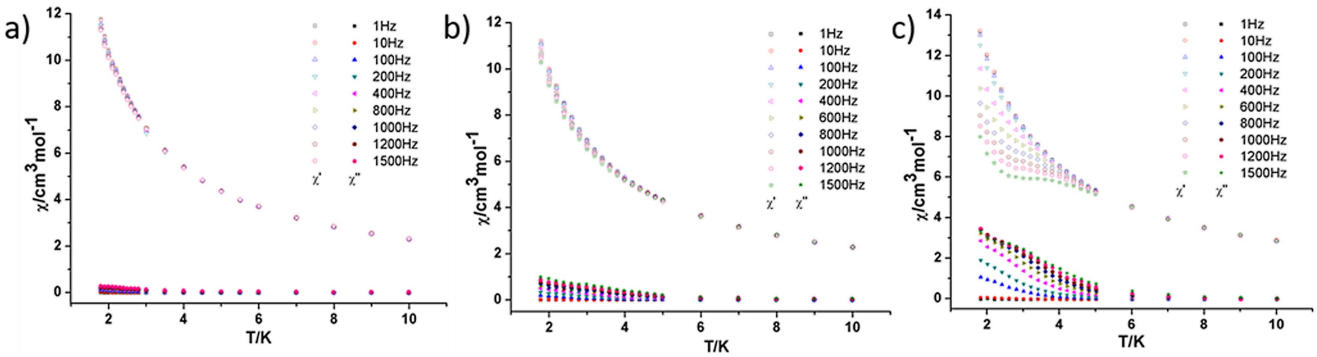

Figure 2. Temperature dependence of the ac magnetic susceptibility under zero dc field for (a) the Fe_2Dy_2 systems with $teaH^{2-}$ as ligand, (b) **1-RS**, and (c) **1-SS**. The out-of-phase data are shown as brighter spots, the in-phase are shown as paler spots.

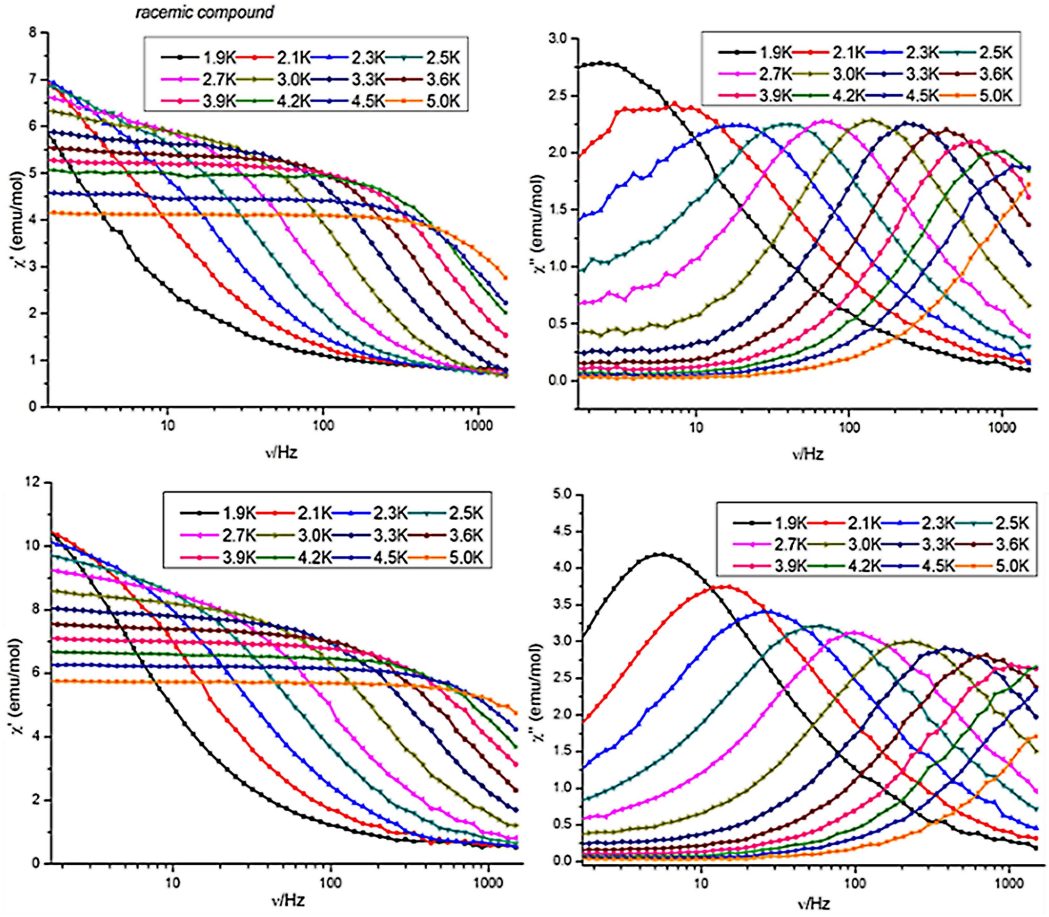

Figure 3. The frequency-dependences of the in-phase (left) and out-of-phase (right) components of the ac magnetic susceptibility for **1-RS** under 2000 Oe dc field (above) and for **1-SS** under 1500 Oe dc field (below).

respective optimum dc fields of 2000 Oe and 1500 Oe. The resulting Arrhenius plots can be found in Figure S12. Barriers of 20.2 K (pre-exponential factor of 1.4 10^{-6} s) and 19.5 K (pre-exponential factor of 1.1 10^{-6} s) were extracted for **1-RS** and **1-SS** respectively. These can be compared to the value of 16.2 K (pre-exponential factor of 1.9 10^{-6} s) obtained for the triethanolamine analogue[4a] (see Table 1).

This shows that changing one arm of the triethanolamine ligand to the methyl substituted version already enhances the U_{eff} by 20% on going from the triethanolamine compound to the *R,S* compound. On the other hand, moving the methyl substituent on going from compound **1-RS** to compound **1-SS** has essentially no effect on the energy barrier U_{eff}. Note that in order to find U_{eff} it is necessary to apply a static *dc* field. Much more informative in terms of gauging the relaxation behaviour is to look at the zero field *ac* susceptibility signals. The striking difference of the behaviour between compound **1-RS** and **1-SS** is the very large enhancement of the zero-field relaxation for compound **1-SS**.

Table 1. . Energy barriers and pre-exponential factors for **1-RS**, **1-SS** and **2-SS** in comparison with the reference compound $Fe_2Dy_2(teaH_3)$[5]

	$Fe_2Dy_2(teaH)_2$[5]	1-RS	1-SS	2-SS
U_{eff}[K]	16.2	20.2	19.5	168
τ_0[s]	1.9×10^{-6}	1.4×10^{-6}	1.1×10^{-6}	3.2×10^{-8}
χ''/χ'	0.025	0.043	0.667	[a]
$J_{Fe\text{-}Fe}$ [cm^{-1}][b]	−5.4	−5.0	−5.0	−5.3

[a] **2-SS** does not show ac signals in zero applied *dc* field, therefore we cannot extract a χ''/χ' ratio. [b] Calculated using magneto-structural based on Ref. [10] using a −2 J model.

Exploration of the properties of the $[Fe_2Dy_2(\mu_3\text{-}OH)_2(Me\text{-}teaH)_2(O_2CPh)_4(NO_3)_2]$ analogues: 2-RS, 2-SS and 2-RR

In the original paper on the Fe_2Ln_2 clusters with $(teaH)^{2-}$ by Murugesu et al.,[5] structures were reported with either six benzoates (as for **1-RS**), or in which the chelating benzoates on the Ln^{III} had been replaced by nitrates. For $[Fe_2Dy_2(\mu_3\text{-}OH)_2(teaH)_2(O_2CPh)_4(NO_3)_2]$,[5] microSQUID data showed very fast quantum tunnelling at zero field. We therefore decided to look at structural analogues with $(Me\text{-}teaH)^{2-}$, in which the two chelating benzoates on the Dy are replaced by two chelating nitrates, to investigate whether the symmetry-breaking found between **1-RS** and **1-SS** could suppress this tunnelling. With appropriate changes to the synthetic method, we could obtain cleanly all three variations (**2-RS**, **2-SS** and **2-RR**), with no racemisation observed for the latter two.

At applied fields between 500–3000 Oe **2-RS** showed no maxima (Figure S14a), in the same field range both **2-SS** and **2-RR** show a maximum for an applied field of 1000 Oe. (Figure S14b and c) Under an applied field of 3000 Oe the **2-SS** compound shows a more complicated behaviour with a maximum that is well within the frequency window. This maximum at 3000 Oe is missing for **2-RR** and instead the best field to observe a maximum is at 1000 Oe. (Figure S14c) Since the corresponding maximum can also be observed for compound **2-SS** we first compared the data under an applied field of 1000 Oe for both **2-SS** and **2-RR** (Figures S15 and S16). Figures S15 and S16 are virtually superimposable.

When we investigated the situation for an applied field of 3000 Oe for **2-SS** (Figure S17) two relaxation processes were observed up to 3.6 K. One is at the lower frequency around 100 Hz, the other at high frequency (over 1500 Hz) which is outside the measurement window of the magnetometer.

The Cole-Cole plots can be fitted using a two relaxation pathway Debye model,[11] with α parameters in the range 0.13–0.42 for low frequency and 0.46–0.70 for high frequency between 2.4 and 3.4 K, indicating a wide distribution of relaxation times. From these fittings, relaxation times at different temperatures are extracted. The resulting Arrhenius plots can be found in Figure S18 from 2.4–3.4 K with an energy barrier of 16.8 K and pre-exponential factor of 3.2 10^{-8} s. This is below the value that was found for both **1-RS** and **1-SS**. For **2-RR**, it was not possible to extract an energy barrier from the data. (see Figure S17) However, the most striking difference is the very large enhancement of the zero-field relaxation behaviour for **2-RR** and **2-SS** compared to **2-RS**. This remarkable switching on of SMM behaviour for the enantiopure systems seems to be a result of having broken the symmetry within the compound. We can observe significant change in the SMM behaviour for **1** and **2**, either improving the dynamic magnetic behaviour (**1**) or enabling slow relaxation of magnetisation in the first place (**2**).

Conclusions

Two Fe_2Dy_2 coordination cluster systems were prepared by using either racemic (*R*,*S*)-Me-teaH$_3$ or the enantiomerically pure (*S*)-Me-teaH$_3$ and (R)-Me-teaH$_3$ ligands. Using the racemic ligand yields the centrosymmetric (*R*, *S*)-Fe_2Dy_2 (**1-RS**) compound, the use of the *S* enantiomer gives the first homochiral 3d/4f SMM (*S*,*S*)-Fe_2Dy_2 (**1-SS**), while for the (*R*)-Me-teaH$_3$ ligand we observe significant racemisation. Compound **1-RS** crystallises in the centric space group $P\bar{1}$ and **1-SS** in the acentric Sohncke space group P1, compatible with the structure's enantiopurity.

The main structural difference between **1-RS** and **1-SS** is the removal of the inversion centre in compound **1-SS**. This has the effect of relaxing all the structural constraints and leads to an enhancement of the magnetic relaxation in compound **1-SS** as shown in the zero field ac susceptibility measurements. These results are further substantiated by the analysis of a second type of butterfly system $Fe_2Dy_2(\mu_3\text{-}OH)_2$(Me-teaH)$_2$(O$_2$CPh)$_4$(NO$_3$)$_2$ (**2**) where breaking symmetry by introducing chirality enhances slow relaxation of magnetisation.

Experimental Section

Synthesis

Compound 1-RS: [Fe_3O(O$_2$CPh)$_6$(H$_2$O)$_3$](O$_2$CPh) (0.25 g, 0.242 mmol), Me-teaH$_3$ (0.326 g, 2 mmol) and Dy(NO$_3$)$_3$·6H$_2$O (0.25 mmol, 0.116 g) were dissolved in MeCN/MeOH (25/10 mL). The orange-brown solution was stirred with heating at 50 °C for 35 min and then left to cool in a closed vial. Crystallisation started after 12 h and the crystals were collected after two days (Yield 84%).

Anal. Calc.: C, 47.26; H, 4.45; N, 4.99%. Found: C, 47.80; H, 4.46; N, 4.88%. Selected IR data (cm^{-1}): 3361 (br), 3064 (w), 2970 (w), 2853 (br), 2502 (w), 2251 (w), 1687 (m), 1596 (s), 1549 (s), 1491 (w), 1450 (m), 1389 (s), 1315 (m), 1267 (m), 1175 (m), 1123 (m), 1090 (m), 1037 (w), 1024 (w), 897 (m), 864 (w), 790 (w), 718 (s), 687 (m), 674 (m), 588 (m), 521 (w), 452 (w), 431 (w).

Compound 1-RR and 1-SS: [Fe_3O(O$_2$CPh)$_6$(H$_2$O)$_3$](O$_2$CPh) (0.25 g, 0.242 mmol) and Dy(NO$_3$)$_3$·6H$_2$O (0.25 mmol, 0.116 g) were dissolved in 10 mL of MeCN. To this was added a solution of *S*-Me-teaH$_3$ or *R*-Me-teaH$_3$ respectively (0.326 g, 2 mmol) dissolved in 5 mL MeCN. The solution was stirred and MeCN (10 mL) was subsequently added followed by the addition of MeOH (10 mL). The orange-brown solution was stirred with heating at 50 °C for 35 min and then left to cool in a closed vial. Crystallisation of 1-SS started after 5–7 days and the crystals were collected after one week (Yield 26%). Crystallisation of 1-RR proved to be more difficult and only a few crystals suitable for single crystal structure determination were obtained.

Anal. Calc.: C, 47.26; H, 4.41; N, 4.99%. Found: C, 47.80; H, 4.46; N, 4.88%. Selected IR data (cm^{-1}): 3361 (br), 3064 (w), 2970 (w), 2853 (br), 2502 (w), 2251 (w), 1687 (m), 1596 (s), 1549 (s), 1491 (w), 1450 (m), 1389 (s), 1315 (m), 1267 (m), 1175 (m), 1123 (m), 1090 (m), 1037 (w), 1024 (w), 897 (m), 864 (w), 790 (w), 718 (s), 687 (m), 674 (m), 588 (m), 521 (w), 452 (w), 431 (w).

Compound 2-RS: A mixture of Me-teaH$_3$ (0.163 g, 1 mmol) and Dy(NO$_3$)$_3$·6H$_2$O (0.25 mmol, 0.116 g) in MeCN/MeOH (10/2.5 mL) was added to a solution of [Fe_3O(O$_2$CPh)$_6$(H$_2$O)$_3$](O$_2$CPh) (0.125 g, 0.121 mmol in MeCN (10 mL) under stirring. The orange-brown solution was stirred for 20 min and then left to a closed vial. Crystallisation started after one day and the crystals were collected after two days (Yield 72%).

$C_{52}H_{72}Dy_2Fe_2N_8O_{24}$ *Anal.* Calc.: C, 38.32; H, 4.45; N, 6.88%. Found: C, 38.16; H, 4.34; N, 6.95%. Selected IR data (cm^{-1}): 3510 (br), 2863 (s), 2492 (w), 1594 (s), 1541 (m), 1380 (m), 1098 (s), 912 (s), 720 (m), 673 (m), 595 (s), 463 (s).

Compounds 2-SS and 2-RR: The same reaction as preparing compound 2-RS, using enantiomerically-pure *S*-Me-teaH3 or *R*-Me-teaH$_3$ replaced racemic ligand Me-teaH$_3$, resulted in enantiomerically-pure compounds, **2-SS** (Yield 51%) and **2-RR** (Yield 46%), respectively. Compound 2-SS. *Anal.* Calc.: C, 38.87; H, 4.20; N, 7.85%. Found: C, 38.77; H, 4.17; N, 7.88%. Compound 2-RR. *Anal.* Calc.: C, 38.87; H, 4.20; N, 7.85%. Found: C, 38.95; H, 4.10; N, 7.74%. Selected IR data (cm^{-1}): 3510 (br), 2863 (s), 2492 (w), 1594 (s), 1541 (m), 1380 (m), 1098 (s), 912 (s), 720 (m), 673 (m), 595 (s), 463 (s).

Control measurements: The enantiopure *S*-1-[N,N-bis-(2-hydroxyethyl)-amino]-2-propanol (Me-teaH$_3$) ligand was synthesised according to the literature method.[12] Chromatograms from chiral HPLC are shown in Figures S1–S3. Those in Figures S1 and S2

confirm the absolute configurations of the ligands. In Figure. S3, the chromatogram of the mother solution from compound **1-SS** is shown in order to demonstrate that the remaining ligand in solution after collecting the crystals still has the absolute configuration *S*. Figure S4 shows the CD spectrum of **1-SS** measured in THF solution (0.125 M), which further confirms the homochirality of **1-SS**.

Magnetochemistry: Magnetic susceptibility data (1.8-300 K) were collected on powdered samples restrained in eicosane to avoid orientation problems using a Quantum Design MPMS-XL SQUID magnetometer with an applied field of 0.1 T. Magnetisation isotherms were collected between 0 and 7 T at 2, 3 and 5 K. *ac* magnetic susceptibility measurements were performed for both compounds with *dc* fields from 0 to 3000 Oe and frequencies between 1 to 1500 Hz and 1.8 to 10 K.

Crystallography: Crystallographic data for the structures are summarised in Table S1.

Deposition Numbers 1058715 (for **1-RS**), 1058716 (for **1-SS**), 2101856 (for **1-RR**), 2101853 (for **2-RS**), 2101854 (for **2-SS**), 2101855 (for **2-RR**) contain the supplementary crystallographic data for this paper. These data are provided free of charge by the joint Cambridge Crystallographic Data Centre and Fachinformationszentrum Karlsruhe Access Structures service.

Acknowledgements

This work was supported by the DFG-funded transregional collaborative research centre SFB/TRR 88 "3MET". We acknowledge the Synchrotron Light Source ANKA and Dr. Gernot Buth for provision of instruments at the SCD beamline for the structure determination of compound **1-SS**. AB and AKP acknowledge and support from the STN programme of the Helmholtz Gemeinschaft. NL thanks the Alexander von Humboldt foundation for the financial support. Open Access funding enabled and organized by Projekt DEAL.

Conflict of Interest

The authors declare no conflict of interest.

Keywords: Chirality · cooperativity · dysprosium · iron · single-molecule magnets

[1] a) L. D. Barron, *Nat. Mater.* **2008**, *7*, 691–692; b) C. Train, R. Gheorghe, V. Krstic, L.-M. Chamoreau, N. S. Ovanesyan, G. L. J. A. Rikken, M. Gruselle, M. Verdaguer, *Nat. Mater.* **2008**, *7*, 729–734; c) C. Train, M. Gruselle, M. Verdaguer, *Chem. Soc. Rev.* **2011**, *40*, 3297–3312; d) N. Hoshino, F. Iijima, G. N. Newton, N. Yoshida, T. Shiga, H. Nojiri, A. Nakao, R. Kumai, Y. Murakami, H. Oshio, *Nat. Chem.* **2012**, *4*, 921–926; e) M. Verdaguer, *Nat. Chem.* **2012**, *4*, 871–872.
[2] A. Baniodeh, C. E. Anson, A. K. Powell, *Chem. Sci.* **2013**, *4*, 4354–4361.
[3] H. D. Flack, *Helv. Chim. Acta* **2003**, *86*, 905–921.
[4] a) A. Baniodeh, Y. Lan, G. Novitchi, V. Mereacre, A. Sukhanov, M. Ferbinteanu, V. Voronkova, C. E. Anson, A. K. Powell, *Dalton Trans.* **2013**, *42*, 8926–8938; b) A. Baniodeh, V. Mereacre, N. Magnani, Y. Lan, J. A. Wolny, V. Schünemann, C. E. Anson, A. K. Powell, *Chem. Commun.* **2013**, *49*, 9666–9668; c) V. Mereacre, A. Baniodeh, C. E. Anson, A. K. Powell, *J. Am. Chem. Soc.* **2011**, *133*, 15335–15337.
[5] M. Murugesu, A. Mishra, W. Wernsdorfer, K. A. Abboud, G. Christou, *Polyhedron* **2006**, *25*, 613–625.
[6] H. D. Flack, G. Bernardinelli, D. A. Clemente, A. Linden, A. L. Spek, *Acta Crystallogr. Sect. B* **2006**, *62*, 695–701.
[7] H. D. Flack, G. Bernardinelli, *Acta Crystallogr. Sect. A* **1999**, *55*, 908–915.
[8] T. Yamaguchi, J.-P. Costes, Y. Kishima, M. Kojima, Y. Sunatsuki, N. Bréfuel, J.-P. Tuchagues, L. Vendier, W. Wernsdorfer, *Inorg. Chem.* **2010**, *49*, 9125–9135.
[9] a) M. Pinsky, D. Avnir, *Inorg. Chem.* **1998**, *37*, 5575–5582; b) S. Alvarez, D. Avnir, M. Llunell, M. Pinsky, *New J. Chem.* **2002**, *26*, 996–1009; c) D. Casanova, J. Cirera, M. Llunell, P. Alemany, D. Avnir, S. Alvarez, *J. Am. Chem. Soc.* **2004**, *126*, 1755–1763; d) S. Alvarez, P. Alemany, D. Casanova, J. Cirera, M. Llunell, D. Avnir, *Coord. Chem. Rev.* **2005**, *249*, 1693–1708.
[10] K. J. Mitchell, K. A. Abboud, G. Christou, *Inorg. Chem.* **2016**, *55*, 6597–6608.
[11] a) K. S. Cole, R. H. Cole, *J. Chem. Phys.* **1941**, *9*, 341–351; b) D. Reta, N. F. Chilton, *Phys. Chem. Chem. Phys.* **2019**, *21*, 23567–23575.
[12] a) Y. Kim, Y. Han, J.-W. Hwang, M. W. Kim, Y. Do, *Organometallics* **2002**, *21*, 1127–1135; b) W. A. Nugent, R. L. Harlow, *J. Am. Chem. Soc.* **1994**, *116*, 6142–6148.

Manuscript received: September 14, 2021
Accepted manuscript online: October 7, 2021
Version of record online: October 21, 2021

